SECOND TARGET STATION (STS) PROJECT

CENTAUR Technical Report

Dr. Shuo Qian
Eng. Cristina Boone

Date 3/31/2022

OAK RIDGE NATIONAL LABORATORY

SECOND TARGET STATION (STS) PROJECT

CENTAUR Technical Report

Prepared by: _____
      Shuo Qian, STS SANS Instrument Development Scientist

Prepared by: _____
      Cristina Boone, CENTAUR Lead Engineer

Approved by: _____
      Leighton Coates, STS Instrument and Technical Manager

Approved by: _____
      Kenneth Herwig, STS Instrument Systems Manager

Date Published:

7/26/2022

Prepared by
OAK RIDGE NATIONAL LABORATORY
Oak Ridge, TN 37831-6283
managed by
UT-BATTELLE, LLC
for the
US DEPARTMENT OF ENERGY
under contract DE-AC05-00OR22725

CONTENTS

List of Acronyms

CCR Closed Cycle Refrigerator
DOE U.S. Department of Energy
FWHM Full-Width-at-Half-Maximum
HFIR High Flux Isotope Reactor
Hz Hertz (SI physical unit for frequency)
IC&DAS Instrument control and data acquisition system
McStas Monte Carlo Simulator for triple axis spectrometer
MCViNE Monte Carlo Virtual Neutron Experiment
NIST National Institute of Standards and Technology
ODH Oxygen Deficiency Hazard
ORNL Oak Ridge National Laboratory
PPS Personal Protection System
R&D Research and Development
RMA Radiological Materials Area
SDD Sample-to-Detector Distance
SiPM Silicon Photomultiplier
SNS Spallation Neutron SourceSTS Second Target Station
T Tesla (SI physical unit for magnetic field)
ToF Time-of-Flight
WBS Work Breakdown Structure

ABSTRACT

CENTAUR will be the flagship general purpose small-angle neutron scattering (SANS) instrument for the Second Target Station of SNS. Based on an optimized and high-performance SANS instrument, it is capable of SANS/wide-angle neutron scattering and diffraction simultaneously filling the capability gap to cover structure scale from atomic scale to hundreds of nanometers for scientific needs ranging from polymers, biology, materials sciences, and quantum condensed matter. Additionally, with a high-speed chopper, it can be used as a direct geometry spectrometer to probe the dynamics in relatively large length-scale structures as an inelastic SANS spectrometer. The technical details of the CENTAUR instrument are presented in this document. As the project progresses, the initial details are subject to change based on feedback.

1. SCIENCE CASES

CENTAUR, specifically designed and optimized for construction at the Second Target Station (STS) of the Spallation Neutron Source (SNS) at Oak Ridge National Laboratory (ORNL), is a small- and wide-angle neutron scattering (SANS and WANS) instrument with a large dynamic range in reciprocal space. It will cover length scales from atomic distance (diffraction) to hundreds of nanometers (small-angle scattering) simultaneously and have additional capability as a direct geometry spectrometer to probe the dynamics in a relatively large length-scale structure.

In many science areas, including soft matter, polymer science, geology, biology, quantum condensed matter, and other materials sciences, there is a capability gap to perform in-situ and operando experiments for kinetic and out-of-equilibrium studies of phenomena. Several transformative opportunities have been mentioned, e.g., in recent reports from the Basic Energy Sciences Advisory Committee and National Science Foundation and National Academies of Sciences Engineering Medicine[1–3], such as mastering hierarchical architectures and beyond-equilibrium matter; understanding heterogeneity, interfaces, and disorder beyond ideal materials and systems; and advancing imaging capabilities across multiple scales. CENTAUR is a critical tool developed to fill this capability gap.

As a multipurpose SANS instrument with expanded capability as WANS/diffractometer/spectrometer, CENTAUR can measure almost any sample in any morphology, including solid, liquid, and gaseous state. Here we only very briefly introduced a series of scientific cases from representative user communities. From the science cases, the instrument requirements are derived.

In polymer sciences, the polymer self-assemble process spans six orders of magnitude of time from seconds to days, into hierarchical structure length scales ranging from angstroms to micrometers. This multiscale assembly process determines both the structure and the properties of the material, including mechanical strength, conductivity, and biological activity. Unfortunately, current analytical techniques allow for only a small window of observation in size and time that often does not encompass all the relevant features and processes of interest. CENTAUR is needed to cover the length scales in this observational range from Å to beyond 100 nm and time scales from seconds to days in a single measurement to provide the insight needed to correlate the hierarchical structure progression with the material's assembly mechanism. Some examples of polymer studies requiring such capabilities are (1) helical assembly observed in synthetic biomolecules-mimic polymers, (2) polymer gels and networks including many field-changing innovations such as the invention of double network hydrogels[4] and slide-ring gels[5], (3) polymer phase transition during the industrial processes, (4) poly(ionic liquid)s (PILs)[6,7], an innovative class of polyelectrolytes exhibiting high CO_2 sorption capability and much faster CO_2 capture and desorption rates [8,9].

In material sciences, a good science example is the characterization of the additive manufacturing (AM) process. Compared with traditional manufacturing process, AM is unique in that its processing is often highly nonequilibrium. Thus, the properties of the as-built materials are process-dependent. Understanding material behaviors far away from equilibrium is one of the grand scientific challenges. The nonequilibrium processes used in AM pose significant challenges to the wide-ranging adoption of AM technologies and require that we expand our knowledge base. With neutron's ability to nondestructively penetrate real parts and components, CENTAUR can detect structures with thicknesses above the millimeter level under operational conditions. The groundbreaking time resolution in seconds at CENTAUR removes one major barrier that traditionally limits the impact of neutron scattering instruments in probing materials manufacturing processes, especially those related to materials' transformational kinetics during processing and service.

In geoscience, for example, carbon sequestration in subsurface formations, including hydrocarbon reservoirs, deep coal and shale formations, and saline aquifers, is a viable strategy for storing CO_2 underground permanently. Carbon mineralization is an emerging approach to storing CO_2 in carbonate minerals such as calcite and magnesite to increase CO_2 storage security.[10] Overall, the characterization of

fluid-rock interactions, from the atomic scale to the macro-scale, in host rock formations is essential to understanding the kinetics and the total storage of CO_2 in these targeted formations. The combination of CENTAUR's capabilities with the neutron contrast-matching power will extend previous studies of pore accessibility,[11–13] induced pore deformation,[14–17] and gas behaviors in pores[17–19] at the nanoscale to atomic-scale mineral structure. In addition, CENTAUR offers a wide range of sample environments, including an automatic in-line flow cell, temperature/pressure ramping, humidity control, strain, and shear. Therefore, CENTAUR will be an excellent choice to determine fluid transport and storage behaviors in geomaterials under in situ conditions.

In biology, for example, intrinsically disordered proteins (IDPs) or intrinsically disordered regions (IDRs) in proteins are highly dynamic without well-defined structures. Half of all human proteins are either wholly or partially disordered; they are essential for many biological processes and represent a completely different structural paradigm to be understood. Small-angle scattering is especially useful in understanding their highly flexible structures as other techniques such as crystallography, and cryo-electron microscopy are not applicable for them. One of the important organizing features of IDPs is the formation of membrane-less organelles within the cell through the liquid-liquid phase separation (LLPS) process.[20] The dynamic nature of LLPS with their hierarchical structural organization associated with various pathologies is key to understanding the protein aggregation involved in many diseases. With its enhanced time resolution and extended spatial range, along with the smaller sample volumes required, CENTAUR will advance the structural and kinetical knowledge of IDPs and their complexes. In addition, CENTAUR will be an invaluable tool for understanding such heterogeneous structures and interactions. For example, with the increasing complexity in studying biological membrane and live cell systems,[21,22] the wide dynamic Q range of CENTAUR will provide an omics-level view of systems at length scales up to 100+ nm. The kinetic changes occurring over seconds in temporal resolution in response to stimuli or other environmental factors, which usually are not easily reproducible, can be obtained over all the length scales involved. Phenomena such as photosynthesis converting sunlight into cellular fuel in cyanobacteria and light-induced thylakoid membranes/intracellular organization changes can be studied in greater detail with those capabilities.[23,24]

For quantum condensed matter, a traditional strength of magnetic SANS is the investigation of flux lattices of superconductors and chiral magnetism, including the celebrated skyrmion spin textures.[25,26] The high flux and high resolution of CENTAUR will enable such experiments to be completed quickly and with a new level of precision with high resolution from better $\Delta\lambda/\lambda$ in a TOF source without sacrificing flux. This capability will open up new areas of investigation at this frontier. Another example is the advent of high-throughput entropic mapping of field and temperature space in candidate magnetic materials[27,28] with a host of unexplained states; many of these are proposed to be previously hidden topological spin textures, which likely are distinguishable from one another and from topologically trivial spin configurations only through subtle variations in SANS data. With a smaller sample and higher throughput at CENTAUR, rapidly traversing the (*H*, *T*) phase space of small-volume crystals will provide a breakthrough for the community. Furthermore, the broad *Q* range of CENTAUR will open new possibilities for investigating newly predicted spin textures, such as antiferromagnetic skyrmions,[29] that are not accessible with current SANS instrumentation. CENTAUR will also enable a key new window into understanding the emergent electrodynamics of these spin textures, many of which are sought for potential applications. In this case, understanding the response to time-varying electric and magnetic fields is essential. The time structure of the STS neutron pulse provides an ideal pathway to investigate the dynamics of current and applied field.

CENTAUR will provide capability to measure both structure and dynamics under the same setup, which will significantly accelerate the understanding for many samples. This advance will have a broad impact on research in magnetic materials, as information obtained from inelastic scattering in the first Brillouin zone is particularly rich because of the minimal *Q*-averaging. Such information would be valuable for high-throughput studies at the early stages of the materials life cycle, particularly when it is coupled with data from other spectrometers at STS, like BWAVES and CHESS.[30] This combination will greatly accelerate the investigation and selection of model materials and enhance the impact of neutron scattering investigations on problems in many materials. Another example is water dynamics in a confined

environment. The relaxation dynamics of water in the confinement due to interfacial water can be measured by using neutron Brillouin scattering.[31,32] CENTAUR will extend them further into lower Q-E range to capture the low Q phonon dispersion and decay of low-Q phonon.

2. INSTRUMENT REQUIREMENTS AND DESCRIPTION

2.1 INSTRUMENT REQUIREMENTS DERIVED FROM SCIENCE CASES

As a multi-function instrument with an extensive range of science cases, the optimization and design of CENTAUR must be prioritized. Based on the science and the initial STS eight-instrument suite selection, in which only CENTAUR is SANS-capable, the following order of priorities is adopted:

1. First, CENTAUR is a high-performance SANS/WANS instrument. The minimum Q reachable shall be comparable to most main-stream SANS instruments, e.g., 0.001 Å^{-1}. The WANS capability on the maximum Q requirement varies depending on samples but should be flexible up to 2 Å^{-1}. As the requirement between flux and divergence at samples varies greatly, the instrument configuration needs to be flexible. For example, for many SANS experiments, Qmin and Q resolution can be relaxed to obtain higher flux to archive high temporal resolution. CENTAUR needs to provide a means to achieve the desired configuration with flexibility in the optics system.

2. Secondly, CENTAUR provides diffraction coverage up to 20 Å^{-1}, simultaneously with SANS/WANS measurement, which is important for atomic-scale investigations.

3. As an additional feature, the instrument can be turned into a direct geometry spectrometer for inelastic SANS by inserting a high-speed monochromatic chopper, presumably a Fermi chopper next to the sample position.

With the flexibility in its optics systems and a spacious sample area, CENTAUR offers an array of sample environments ranging from high-throughput sample changers to high-field magnets, as well as beam polarization capability. The high-level instrument specifications derived from the science cases are listed in Table 1.

Table 1. High-level instrument specifications

Sample size	Typical radius 1–5 mm, other shapes possible with different apertures, e.g., 4×8 mm^2, or smaller; minimum static solution sample in volume: ~100 μL; 1×1 mm^2 for scanning imaging or tomography	
Q range	Maximum dynamic range 0.001–20 Å^{-1} simultaneously. Variable Q range with different flux/divergence settings.	For example: Typical solution scattering: 0.001-2.0 Å^{-1} Typical moderate-ordered sample: 0.001-6 Å^{-1} Typical diffraction samples: 0.001-20 Å^{-1}
Detector Coverage	Coverage of the maximum Q range simultaneously without repositioning	
Wavelength bandwidth	7.4 Å (15 Hz), 14.8 Å (7.5 Hz)	
Q resolution ($\Delta Q/Q$)	Forward detectors (small- and wide-angle): < 10% Backscattering detectors (diffraction): < 1%	
Time resolution	>1 second (with moderate scattering samples)	
Additional capability	Inelastic SANS spectrometer (Incident energy E$_i$: 0.5-500 meV) Polarized analysis up to 0.3 Å^{-1}	

|	
Sample environment	Walk-in sample space, convenient sample environment device changes. Wide range of sample environments: SANS sample cells, automatic sample changers, automatic in-line flow cell, liquid handling robot, temperature/pressure/humidity control, flow-through size-exclusion chromatography, stroboscopic sample environment capability, other in situ cells as needed, e.g., stain, shear; closed-cycle refrigerators, low-temperature cryostats, including ^{3}He and dilution refrigerators, and magnets

2.2 KEY INSTRUMENT COMPONENTS

CENTAUR is a linear instrument in which the sample will be in direct view of the neutron source. The instrument will be located at STS source ST06, which is 3 cm-diameter tube coupled para-hydrogen moderator with high brightness and integrated flux within the useable wavelength band. Primary CENTAUR instrument components and their locations are listed in Table 2. The current instrument design is presented in Figure 1. Key instrument components are also presented in Figure 2 with locations labeled.

Table 2. Key component location and length

Component	Starting location from the source (m)	Length (m)	Ending position from the source(m)	Note
Source ST06			0	3-cm tube moderator
Monolith insert guide	0.78000	1.21900	1.99900	
Guide	2.00000	4.21379	6.21379	
Chopper 1	6.24629	0.04050	6.28679	
Guide	6.28679	1.50000	7.78679	
T0 Chopper	7.78679	0.44800	8.23479	
Guide	8.23479	1.42160	9.65639	
Chopper 2	9.68549	0.0839	9.76939	
Guide	9.76939	3.51891	13.28830	Through the bunker
Guide (Operations shutter)	13.28830	1.14290	14.43120	
Guide	14.46320	1.0	15.46320	
0-Guide source aperture (translatable)	15.47920			Variable Optics System
Variable guide 1 (translatable)	15.47920	3.0	18.47920	
1-Guide source aperture (translatable)	18.47920			
Variable guide 2 (translatable)	18.47920	3.0	21.47920	
2-Guide source aperture (translatable)	21.47920			
Variable guide 3 (translatable)	21.47920	1.0	22.47920	
3-Guide source aperture (translatable)	22.51120			
Fermi chopper (translatable)	22.70000			
Sample aperture (translatable)	25.45320			
Nominal sample position	25.46320			Sample-to-detector distance
High-angle detector array	26.57420			1.111 m
Mid-angle detector array	28.79620			3.333 m
Low-angle detector array	35.46320			10.0 m
Backscattering detector array	24.21320			-1.25 m
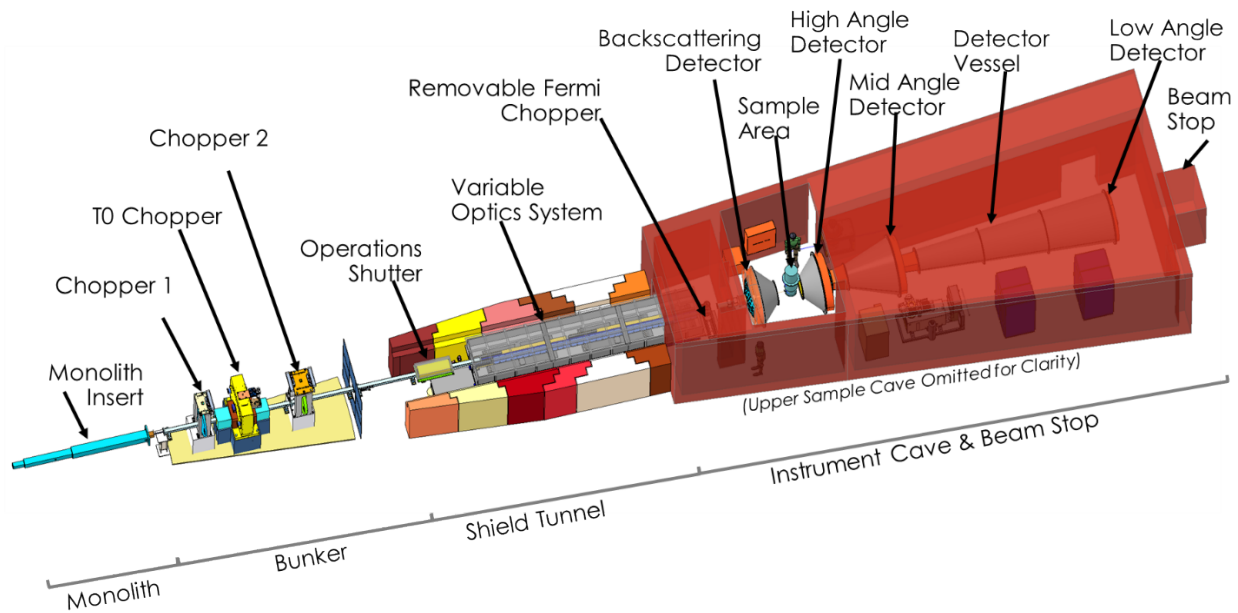
(A)
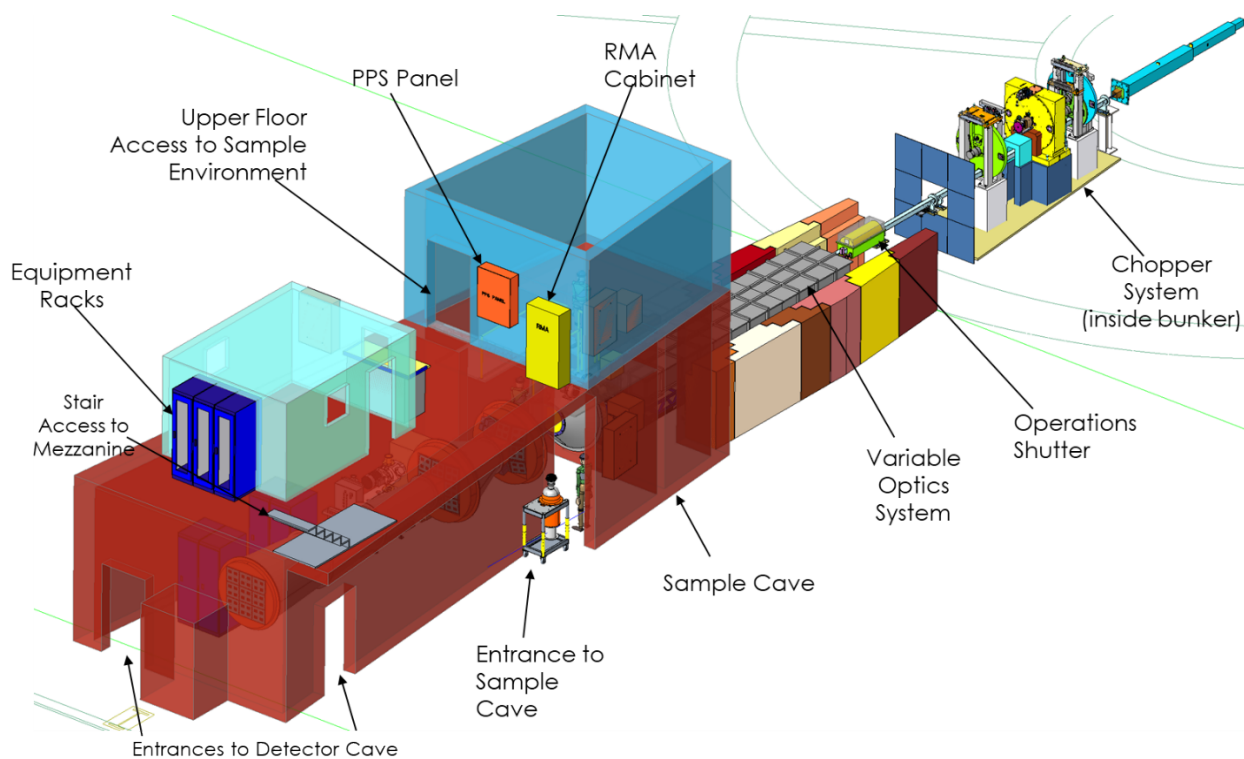
(B)

Figure 1. Isometric view of CENTAUR (Many shielding structures such as Monolith Wall, Bunker Wall Shield Tunnel cover are now shown for clarity). (A) View from front (B) View from back.
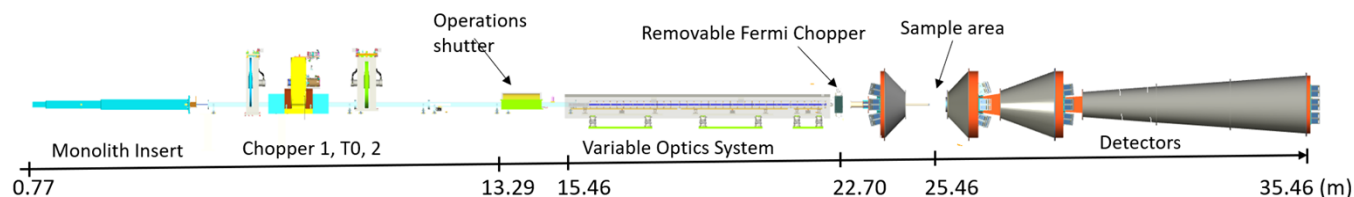
Figure 2. Key instrument components of CENTAUR.

2.3   OPTICS (WBS: S04.07.02)

The optics system includes (1) sections of fixed straight neutron guide, including monolith insert guide, guides between choppers and through the operations shutter's opening position (Figure 2) (2) A variable optics system to provide different collimation distance to adjust flux and divergence. CENTAUR will include provisions to support neutron polarization analysis.

2.3.1   FIXED GUIDES

Inside the monolith insert, a fixed neutron guide will be in place to bring neutrons from the source. Other fixed guides will fillthe gaps between different components such as choppers, the bunker wall and the operations shutter. Neutron guides throughout will be straight supermirrors (m=3) with square openings of 3 by 3 cm to match the source size. McStas simulations were performed as a function of the m-value and cross section size of the guides used in the optics system, including the upstream guide sections, to determine the best m-value. With a typical sample size of 5 mm in radius, using square cross section other than 3 by 3cm significantly reduces the flux at the sample position. Additionally, using m>3 supermirrors doesn't improve the performance at all. m<3 supermirror results in a loss of shorter wavelength neutrons. m=3 mirrors are therefore the preferred choice for balanced performance and cost.

2.3.2   VARIABLE OPTICS SYSTEM

A variable optics system will include interchangeable components, such as neutron guides, open space, and source defining apertures (Figure 3). The system consists of 3 interconnected vacuum boxes based on the proven HFIR SANS collimation box design that was derived from the original NIST SANS design.
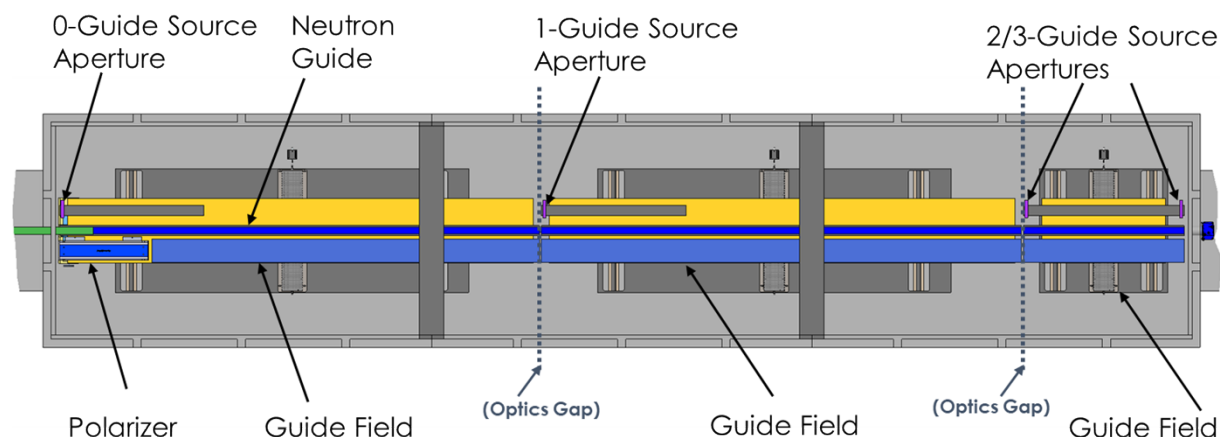

Figure 3. A top view of Variable Optics System.

- The first and the second optic system boxes will be 3 m in length and the last one will be 1 m in length.

- In each box, the interchangeable components are sitting on individual motorized stages for inserting into the neutron beam path as necessary. Three sections of neutron guide with lengths of 3 m, 3 m, 1 m can be inserted into the beam path to provide different collimation and source-to-sample distances of 10 m, 7 m, 4 m and 3 m (designated as Number of Guide (NG) =0, 1, 2, 3, respectively). This is the major mechanism to adjust the flux and divergence on the sample.
- A polarizing supermirror will be in the first box as one of the removable optics components. A magnetic guide field will be present along the beam path to the sample position. The description of the polarization system is detailed in the next section.
- The source apertures, as part of the variable optics system, will be mounted at various places in the vacuum boxes and can be inserted at the end of the neutron guide or the Fermi chopper. They will be 30 mm in diameter to match the sizes of the neutron guides. Additional smaller ones can be provided with reserved positions along the beam path.
- After the last source aperture, an evacuated flight tube will extend the beam to the nominal sample position.

2.3.3 NEUTRON POLARIZATION SYSTEM

The polarization system will fill a capability currently lacking in the ORNL SANS instrument suite. Based on the science drivers, the required Q range for polarization analysis is 0.002 Å^{-1} to 0.3 Å^{-1} under a magnetic field higher than 1 T. Typical sample environments will be closed-cycle refrigerators (CCRs), low-temperature cryostats including ^{3}He and dilution refrigerators, and sample environment magnets capable of fields to 7 T (note that higher fields will be routine in unpolarized mode). With the requirements, the system will focus on providing polarization for SANS, not WANS and diffraction capability. Typical wavelength band, e.g., 2–9.44 Å with the low-angle and mid-angle detector arrays can provide sufficient Q coverage (Table 3).

Table 3 Scattering angle (2θ) and Q coverage limit with an assumed ^{3}He analyzer w. Q_{min} is 0.0016 Å^{-1} at 9.44 Å neutron with NG=0 guide collimation)

	Maximum 2θ (rad)	Q_{max} with 2 Å neutron(Å^{-1})
^{3}He analyzer (50 cm beam path, 15 cm diameter)	0.15	0.47
Low-angle detector array (at 10 m)	0.063	0.178
Mid-angle detector array (at 3.333 m)	0.19	0.597

The system will consist of these major components:

- A neutron spin supermirror polarizer (m=4 for wavelengths longer than 2 Å) at the first section of the variable optics system box. It will generate a polarized neutron beam being guided through a magnetic guide field to the sample. The cross-section will be 3 by 3 m, the same size as the other neutron guides upstream (Figure 3).
- An adiabatic fast passage spin flipper before the sample position to flip the neutron beam polarization relative to the applied magnetic field at the sample.
- A polarized ^{3}He neutron spin analyzer to measure the polarization of the neutron beam scattered by the sample between the sample position and the detector vessel.

In addition, guide field will bridge those components as appropriate. For simplicity and practicality, especially in reducing the instrument background from auxiliary equipment, an ex situ system will be used.[33] In the ex situ system, multiple ^{3}He cells with different diameters of up to 15 cm can be dropped in and swapped easily during the experiment as needed. For example, with a 70% ^{3}He polarization ratio, the ^{3}He cell can be optimized to provide a good balance between the neutron transmission ratio and polarization ratio within the wavelength band (Figure 4). The compactness of the ex situ system will also provide

improved magnetic shielding and additional distance from the sample environment magnet stray field. A "hot swap" during experiments into polarized mode to quickly check signals, and a subsequent return to unpolarized mode for enhanced scattering intensity, will be possible.
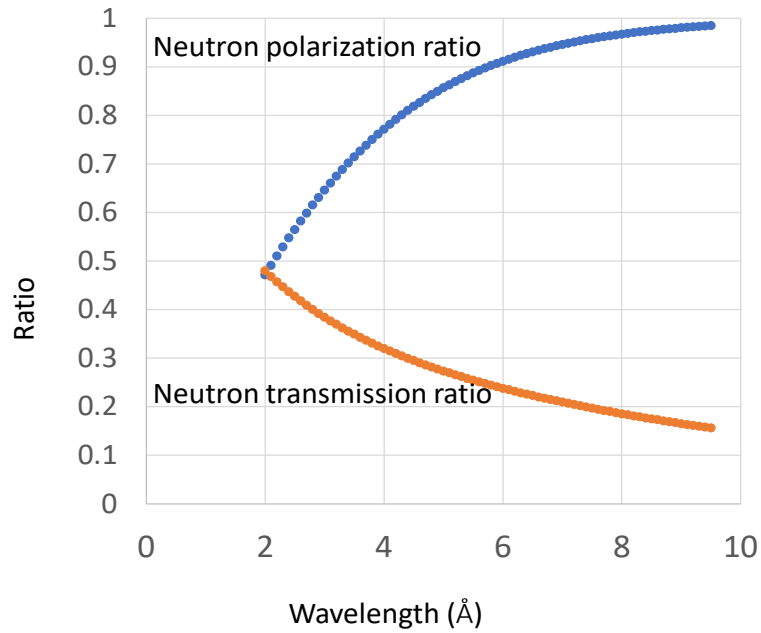

Figure 4. Estimated neutron transmission ratio and polarization ratio at different wavelengths for a ^{3}He cell with a thickness of 5 cm and a pressure of 1 bar with a 70% ^{3}He polarization ratio.

2.4 CHOPPER SYSTEM (WBS: S04.07.03)

- Chopper 1 and Chopper 2 will be bandwidth defining choppers running at 15 Hz or 7.5 Hz (for frame skipping). Using 90% usable bandwidth as an estimate, Chopper 1 and Chopper 2 with the openings 80° and 120°, respectively don't show wavelength leakage up to 70 Å. The estimated transmissions are shown in Figure 5. The bandwidth can be defined by two choppers at one's leading open edge and the other's trailing edge as shown in Figure 6. This combination will allow maximum usable bandwidth. STS large double disc choppers can be used for both. The adjustable opening provided by double disc choppers provides tighter control in bandwidth and minimize the chance of longer wavelength leakage.
- The time-distance diagrams are plotted using the chopper positions and the furthest detector position (35.46 m). At 15 Hz mode, a bandwidth of ~7.44 Å can be achieved, e.g., neutrons from the 2–9.44 Å band (Figure 4A). In the skipped-frame mode of 7.5 Hz, a bandwidth of ~14.88 Å, e.g., 0.5–15.38 Å (Figure 4B), is achievable. The extended wavelength bandwidth greatly extends the dynamic Q range. Increasing the total length, e.g., the furthest detector position, will decrease the usable wavelength bandwidth, reducing the dynamic Q range. In addition, the current furthest sample-to-detector system (10 m) is selected to match the longest collimation distance (10 m) provided the variable optics system. Therefore, the current instrument length of 35.46 m is a balanced choice.
- From Chopper 1 to the starting point of the variable optics system, a number of neutron guide sections will fill the gaps between the components described above to ensure transportation of the neutrons.
- The operations shutter will be located outside the bunker wall. The open configuration of the operations shutter will have a section of neutron guide to ensure full transportation of the neutrons.
- Between Chopper 1 and Chopper 2, an STS large T0 chopper, instead of multi-channel bender guide is used to reduce the fast neutrons and the prompt gramma pulse from the direct view of the moderator. This is required to enhance the signal-to-noise ratio of the instrument. The straight guide with T0

chopper allows significantly more neutron with < 2 Å to reach the sample position (Figure 7). Those shorter wavelength neutrons are crucial to the WANS, diffraction and spectrometer capabilities of CENTAUR. The T0 chopper will need to block neuron < 0.4 Å (> 500 meV).

- A high-speed chopper can be inserted as needed at 22.71 m to provide a spectrometry capability. Due to space constraints, a Fermi chopper will be used. It will be translated out of the beam when it is not in operation.
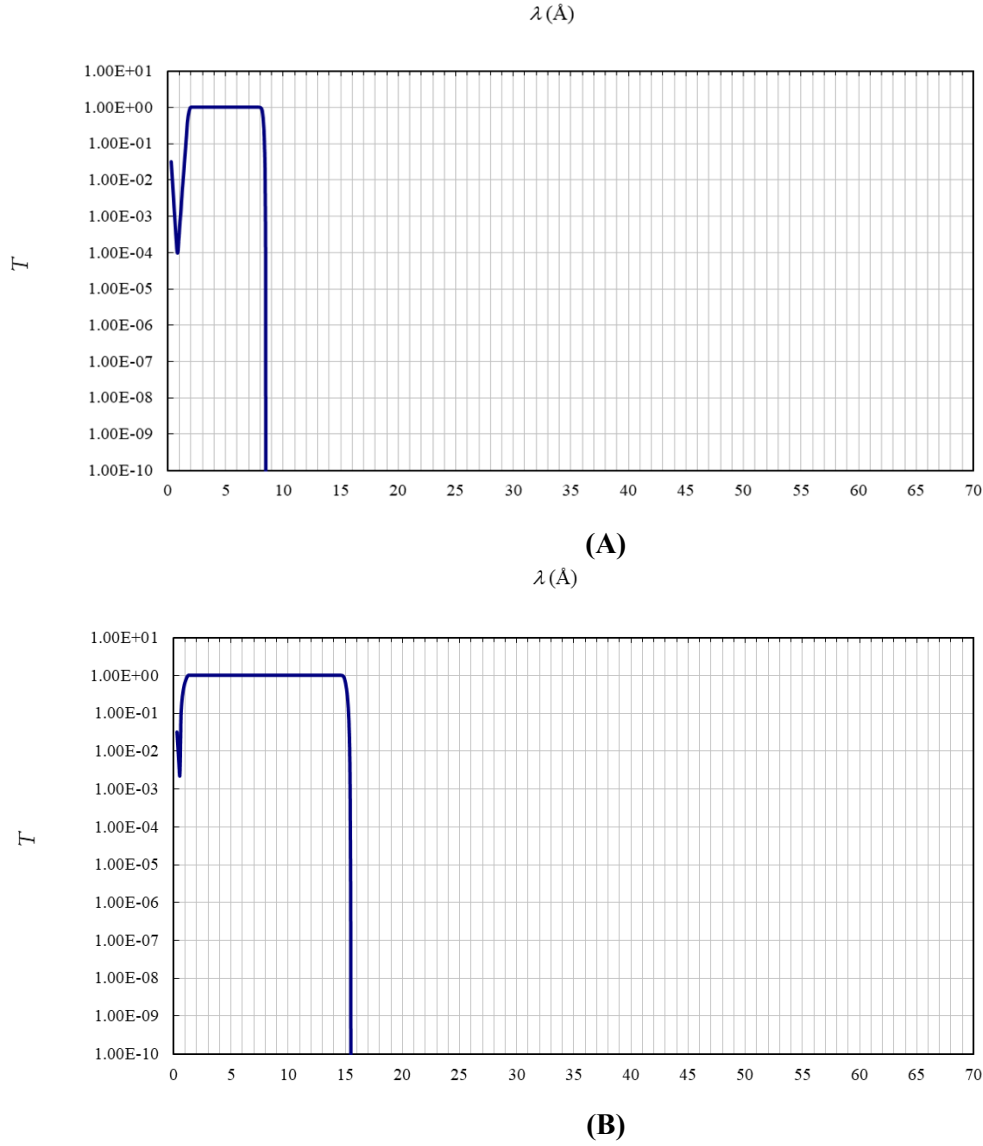
$\lambda\,(\text{Å})$

(A)

$\lambda\,(\text{Å})$

(B)

Figure 5. The chopper transmission from the dual chopper setup for (A) 15 Hz and (B) 7.5 Hz

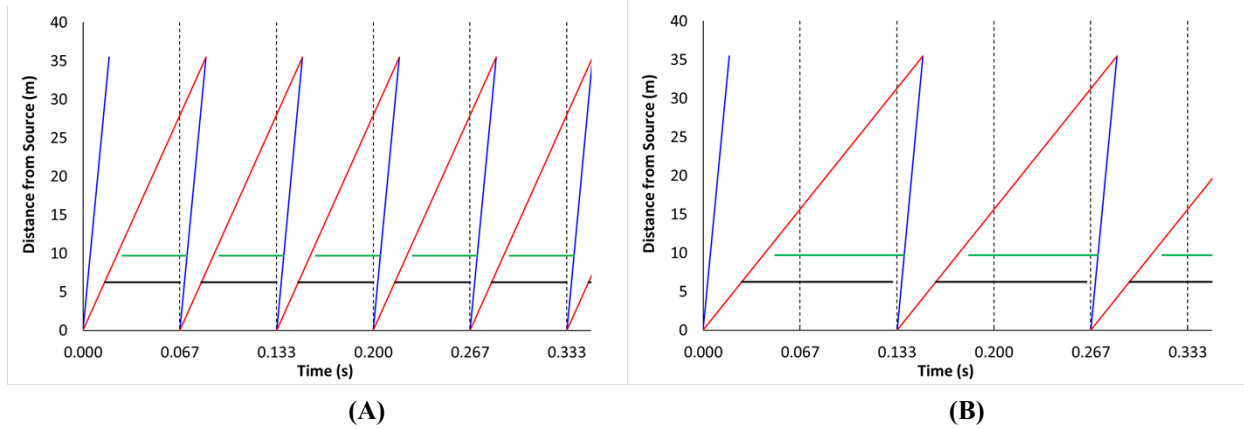**(A)**   **(B)**

Figure 6. Timing diagram examples for selected operation modes: (A) 15 Hz with a bandwidth of 2–9.44 Å (B) 7.5 Hz with a bandwidth of 0.5–15.38 Å.

(A)   **(B)**
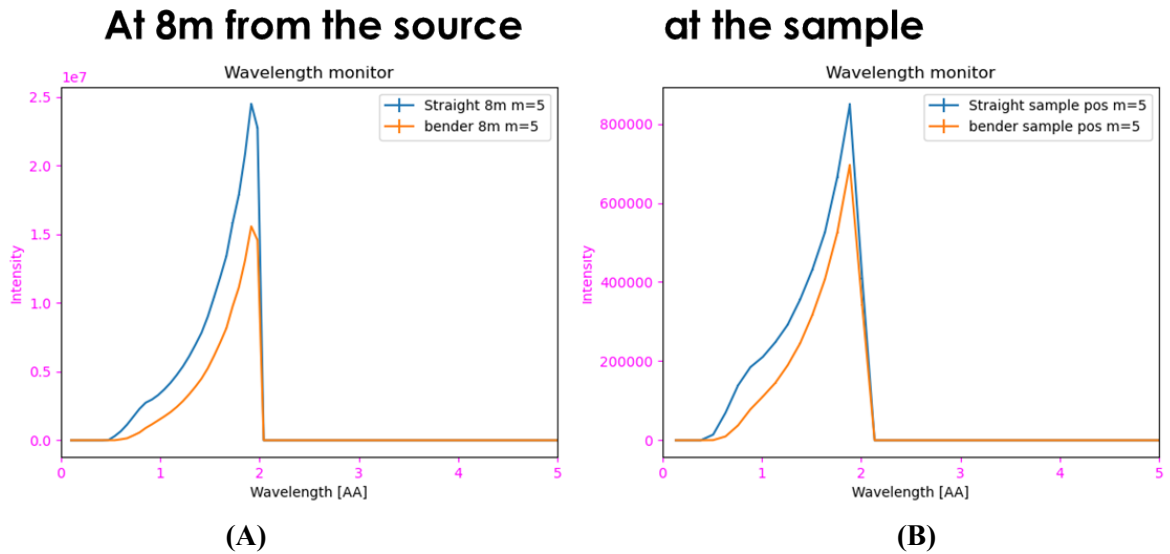
Figure 7. The wavelength band 0.5-2 Å from a straight guide, compared to a bender guide concept of 12 sections of 0.5 m-long straight 3-channel guides angled at 0.092 degrees to each other. (A) at 8 m from the source location; (B) at the nominal sample position.

2.5   SHIELDING (WBS: S04.07.04)

The relatively weak signal in SANS benefits greatly from the reduction of instrument background. Careful shielding and neutron absorbing materials along the optics system, sample cave, and detector vessel/cave are needed to reduce the secondary scattering from strayed neutron and from neighboring instruments to minimize the background (Figure 8). The shielding strategy can be verified by neutronics calculations, if necessary, while the best practice should be exercised within physical and budget constraints during the design process.

13

For the optics system, in addition to the modular concrete outer shielding blocks, additional neutron shielding materials should be integrated as part of the variable optics box. The front end of the optics box structure that the direct beam could hit needs be shielded carefully with neutron absorber, e.g., ^{6}Li containing material. Other parts of the box should be lined with borated material as needed. This ensures that neutrons do not strike structural material of the collimator guide assembly such as steel or aluminum, which gives rise to significant neutron scattering and neutron activation.

The downstream end of the optics box also needs additional shielding to prevent neutrons from reaching the sample area or the detector. The shielding will be designed for neutron optical compatibility with the beam defining aperture system, the neutron guides, Fermi choppers and other likely optical components.

The background from the sample area needs to be minimized. In the final sample beam defining aperture design, considerations should be given to minimize neutron outside the beam path. The air gap between the aperture, sample, and detector vessel window should be minimized or filled with He-gas to reduce air scattering as much as possible.

The neutron detectors need to be shielded. A detector vessel case with high density concrete wall may provide enough shielding from the neighboring instruments. But if that is not enough according to neutronics calculations, an additional shielding layer on the detector backend may be needed. The detector vessel interior should be lined with a layer of neutron absorbing material to reduce secondary scattering from the vessel body material and any background from the sample area.

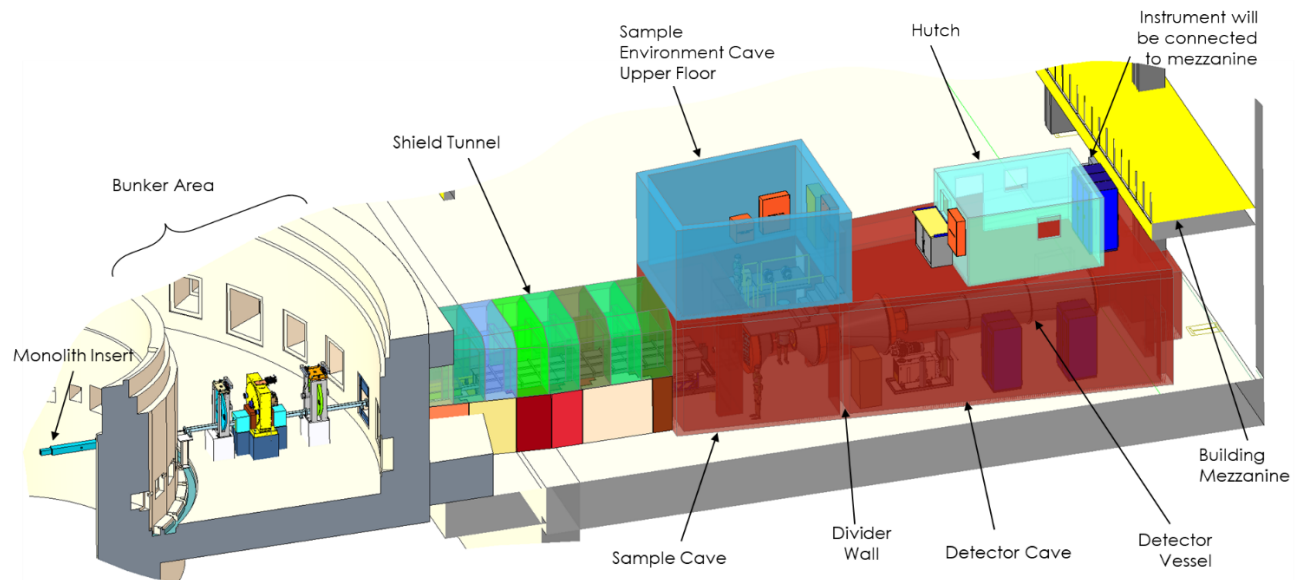**Figure 8.** An isometric view of CENTAUR with the major shielding compoments (Bunker Area, Shield Tunnel, Sample Cave, Detector Cave, etc.)

2.6   DETECTORS (WBS: S04.07.05)

The detectors will be scintillator-Anger cameras with silicon photomultiplier (SiPM detector) modules with a pixel size of 3 mm by 3 mm, matching the most common sample size. Each module will have an active area of 30 by 30 cm.

2.6.1 DETECTOR LAYOUT

There are four arrays of detectors: three arrays in a forwarding direction— the high-angle, mid-angle, low-angle arrays; the 4th array is in a backscattering direction (Figure 9). In the forward direction, the three arrays are at sample-to-detector distance (SDD) 1.111 m, 3.333 m, and 10.0 m. They will be fixed in position without any motion system. A manual adjustment system will be in place for initial installation alignment. The backscattering array is at -1.25 m from the nominal sample position. It can be moved away from its location to provide convenient access for servicing the detector modules. The low-angle array represents the longest neutron path in the instrument (35.46m), determining the maximum usable wavelength bandwidth 7.4 Å (15 Hz) or 14.8 Å (7.5 Hz).
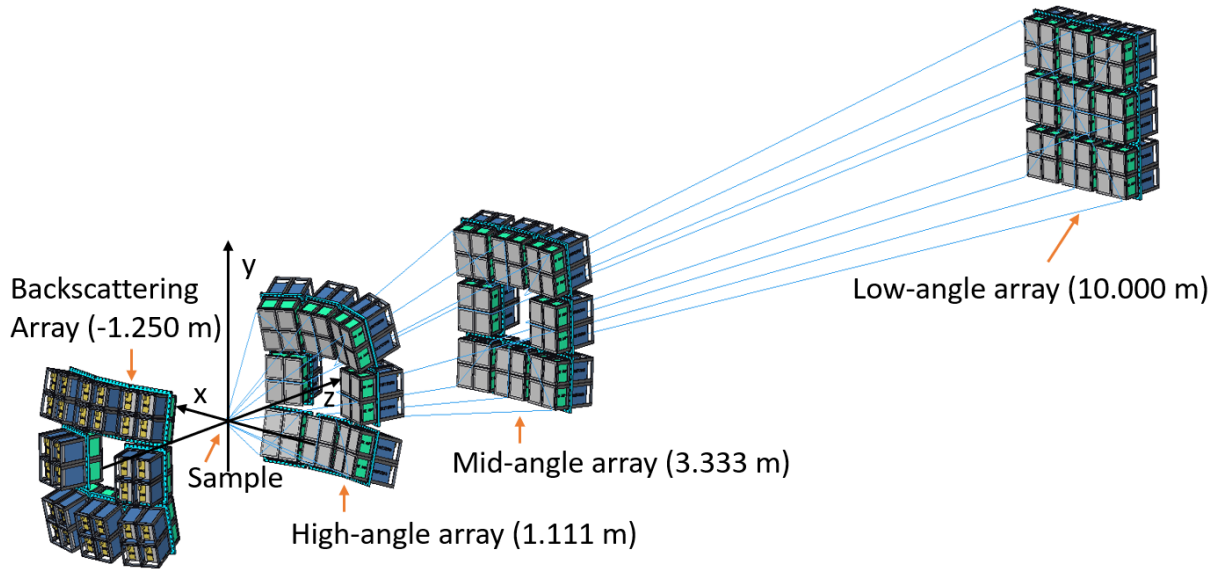

Figure 9. Detector layout in the current preliminary design. The light blue lines illustrate how the rays from the sample position reach different detector arrays. The nominal sample position is shown here, with the SDD labeled.

The detector arrangement and the broad wavelength band are key to providing a large dynamic Q range simultaneously. The gaps between each detector module are usually a few cm. However, the wide wavelength band ensures the overlap of data in Q space. Also, the Q overlaps are sufficiently large between the arrays due to the wide wavelength band and large angular detector coverage. The holes in the high-angle and the mid-angle arrays are optimized to minimize shadowing onto the next array. Again, the wide wavelength band ensures the Q overlap between detector arrays. The modular nature of the detector and high redundancy in the layout geometry will greatly reduce the downtime of the instrument, in case a detector module malfunctions during operation. They can be swapped out for maintenance if necessary. Their coordinates are listed in Table 4.

- **The low-angle array** will be at SDD = 10 m. Nine modules will be in a 3 by 3 module square arrangement with the active areas in a flat surface centered on the direct beam.
- **The mid-angle array** will be arranged on a SDD = 3.333 m radius sphere. The surface of each module is tangent to the sphere, and the center of module is 3.333 m to the nominal sample position. The eight modules will be arranged in a 3 by 3 square array with a missing center module opening to the low-angle array.

- **The high-angle array** will be arranged on a SDD = 1.111 m radius sphere. Similarly, the surface of each module is tangent to the sphere, and the center of module is 1.111 m to the nominal sample position. The eight modules will be arranged in a 3 by 3 square array with the missing center module opening to the low-angle array.
- **The backscattering array** will be arranged on a SDD = -1.25 m radius sphere. The surfaces of the active areas will be tangent to the sphere. There will be eight modules in the backscattering array, arranged in a 3 by 3 square array that is missing a center module that would otherwise be centered on the beam.

Table 4. Coordinate of the detector modules according to current design. The sample location is designated as (0, 0, 0) with conventions of axis shown in Figure 9. Only one set of detectors at corner and side are tabled and the others can be determined from symmetry operations. φx, φy, φz are rotations around x, y, z respectively

Module location	x (m)	y(m)	z (m)	φx	φy	φz
High-angle corner	0.34068	0.34068	1.001097	18.79°	-17.86°	2.98°
High-angle side	0.34885	0	1.05481	18.30°	0°	0°
Mid-angle corner	0.36259	0.36259	3.29332	6.27°	-6.27°	0°
Mid-angle side	0.365	0	3.313	6.27°	0°	0°
Low-angle corner	0.33	0.33	10.00	0°	0°	0°
Low-angle side	0.33	0	10.00	0°	0°	0°
Backscattering corner	0.34	0.34	-1.1538	15.7833°	-15.7833°	0°
Backscattering side	0.34	0	-1.2029	15.7833°	0°	0°

- To provide SEMSANS capability, a high-resolution detector module can be mounted as the central module for the low-angle array at 10 m or an additional retractable detector near that position will be used. The resolution of the detector needs to be 0.2 mm by 0.2 mm and will be part of the Detector R&D program.
- Beam traps of various sizes to block the direct beam before the detector, will be mounted on motion-controlled supports for easy alignment. Semi-transparent beam stops will be developed to provide simultaneous collection of scattered and transmitted neutron beam through the sample.

2.6.2   MONITORS

CENTAUR will use a set of monitors at various locations such as after choppers, in variable optics system to check flux and wavelength (TOF) for diagnostic purpose. The experimental data will be normalized with the proton charge and the monitors will therefore be retracted away during an actual experiment. More details can be found in the document *STS detector needs for STS instruments S04000000-TRT10000.*

2.7   MOTION SYSTEMS (WBS: S04.07.06)

The position of various component along the beamline is controlled by CENTAUR's motion systems. In addition to the motions sytems associated with the standard Maintenance Shutter and the standard Operations Shutter, other instrument specific motion systems will be in place:

- The motion system in the variable optics system will translate different components in/out of beam, and perform alignment of the components.
- The beam traps that block or attenuate direct beam on the detector during the measurement will be mounted on a motion system for individual alignment and utilization.
- Motion systems will be required to control the position and alignment of sample apertures, beam attenuators, removable Fermi chopper, and sample alignment infrastructure equipment. Details of the additional motion systems will be defined during preliminary design of the corresponding systems.

2.8   INSTRUMENT-SPECIFIC (WBS: S04.07.07)

2.8.1   DETECTOR VESSEL

The post-sample scattering path will be in vacuum, provided by a large chamber for all forwarding detectors and a much smaller vacuum or He-gas chamber for the backscattering detectors. Testing of SiPM detectors in vacuum is planned to take part in 2022 as part of the Detector R&D program. As all the detectors are at fixed positions during the measurement, there is no need for a detector motion system, simplifying the design and operation of the instrument. The detector modules will be integrated to a machined vacuum flange that allows the front-end detector sensors to sit inside the vacuum chamber, while the back-end heat-generating detector electronics sit outside the vacuum boundary in air. This concept provides access for detector maintenance while facilitating heat dissipation. As a result, a vessel system as shown in Figure 10 is currently being designed.

Low-angle array

Backscattering array

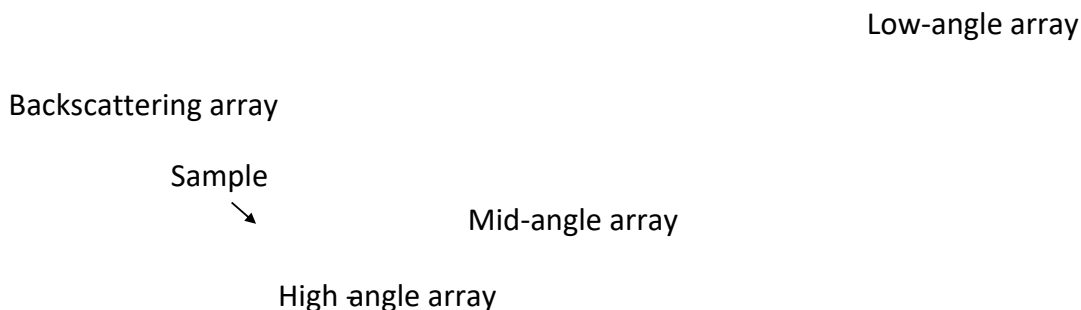Sample

Mid-angle array

High angle array

Figure 10. Current preliminary design of the detector vessels. The detector modules are mounted on the orange plate individually with a large part of their electronics in air. The detecting surface will be in vacuum. The forward vessel is interconnected between different sections in the same vacuum without windows.

17

2.8.2 OPTICAL ALIGNMENT SYSTEM

A light-illuminated alignment aiding system will be developed to align and provide position information for the sample. With the quick swapping modular sample setup, this system will greatly reduce the need to use neutrons to align samples. The alignment system will also inform and update the offset distance between the actual sample position to the nominal sample position in the instrument control software, which is important for accurate data reduction. It will be located in the sample environment area described in Section 2.9.

2.9 SAMPLE ENVIRONMENT (WBS: S04.07.08)

As a general purpose and work-horse SANS instrument with additional capabilities, a large number of sample environment devices are envisioned for CENTAUR. Compared to what has been deployed at the existing SANS beamlines, in general, a much higher throughput and smaller sample footprint are expected for many types of samples. To make time-resolved and/or in-situ or operando measurements, novel sample environment devices need to be developed with the community. Here, we layout an overall consideration and a few example sample environment devices.

2.9.1 SAMPLE POSITION AND GEOMETRY

The nominal sample position will be at 25.463 m from the moderator. Larger sample environment devices may slightly offset away the nominal sample position by a small distance. It will be an open walk-in space inside a radiation-shielded cave. It will offer flexibility for smaller and larger sample environments, such as a robotic sample changer, a cryo-magnet, or a ^{3}He analyzer for polarization analysis. The sample aperture will be positioned immediately before sample. A variable aperture system will provide the flexibility to use different beam sizes from 1 mm to 5 mm in radius and additional shapes and sizes as needed.

Large sample environments will shift the actual sample position slightly depending on their size. In some cases, due to the shadowing from such sample environment, scattering angle and backscattering geometry will be restricted, only allowing for SANS/WANS experiment.

For maximum compatibility between the instrument's diffraction and SANS/WANS capabilities, a typical flat SANS sample geometry is recommended. It was used as the primary test sample geometry in the performance estimations. This geometry has influenced the location and geometry of the detectors, especially the location of the diffraction detectors as a backscattering detector. However, other geometries can be supported depending on the needs of a given experiment.

2.9.2 GENERAL CONSIDERATIONS

CENTAUR needs to maintain compatibility with sample environment devices that are being used or currently under development across the ORNL SANS suites. The walk-in open space currently designed for CENTAUR (Figure 11) provides maximum compatibility and flexibility.

- Modular sample setup: To facilitate quick sample environment change, all designs, but especially the smaller ones (other than magnet, cryogenic equipment) will be modular and can be ready within 1 hour or less for actual experiment. For example, for equipment with size smaller than 1m × 1m × 1m that can be moved around by cart, shall be assembled ahead of time and moved into place for quick change out.
- Sample alignment and positioning device: Sample positioning systems such as a goniometer will provide precise positioning within at least 0.1 mm accuracy for a typical 10 mm sample. The rotation and tile, if necessary, within 0.01° accuracy. The optical alignment system in Section 2.8.2 will aid sample alignment too.

- Video cameras will be installed at various locations to visually monitor samples and sample environment during experiments.
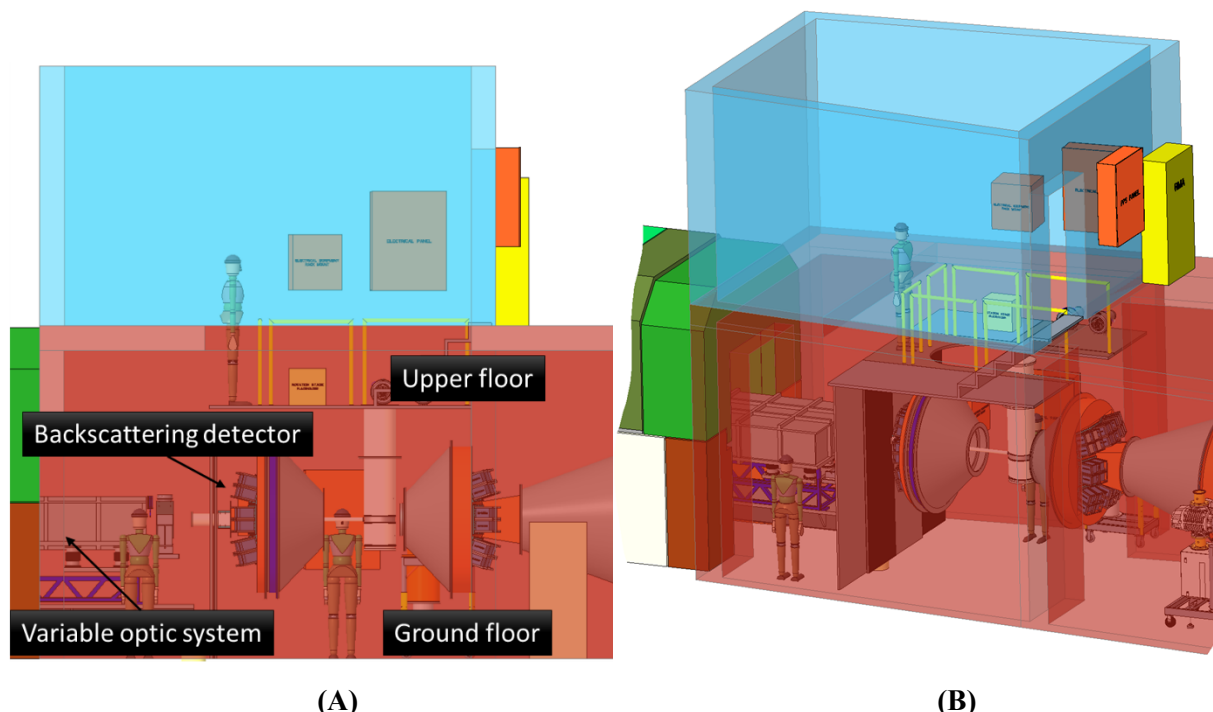

Figure 11. The sample area of CENTAUR. The walk-in ground floor provide access to most sample environment and convenience to swap sample environment. The upper floor provides convenience for top-loading equipment such as cryo-magnets. (A) a side-view (B) an isometric view. The support structures for detector arrays are not shown for simplicity.

2.9.3   MULTIMODAL MEASUREMENT

To provide complementary measurements to neutron scattering to provide a deeper understanding of the complex systems on CENTAUR, multimodal measurement capability will be developed. For example, in situ UV-Vis spectrometry, dynamic light scattering (DLS) and Förster resonance energy transfer (FRET) will provide additional information for many time-resolved phenomenon that cannot be repeated easily. The distributions of particle sizes by DLS and the distribution of short-range distances between specific, labelled moieties greatly complement SANS/WANS/diffraction data from CENTAUR. With similar approaches, additional optical spectrometry methods e.g., Raman can also be implemented, turning the instrument into a 'lab-on-beam' setup.

2.9.4   SAMPLE CHANGER FOR HIGH-THROUGHPUT EXPERIMENT

Currently, most SANS beamlines are using standardized individual sample cells to perform experiments, with the expected high throughput at CENTAUR, different approaches for sample changers are required.

- **Robotic arm sample changer:** with the multimodal sample environment, the typical multi-position sample changer becomes impractical. A robotic arm sample changer will provide almost unlimited sample numbers during an experiment. Additional robotic arms can be implemented to provide versatile sample manipulation near/in beam.

- **Liquid-handling and flow-through sample changer:** Liquid-handling robots will provide another lab-on-beam capability to titrate or change samples during an ongoing experiment. Flow-through sample changer, as a standard setup among many small-angle X-ray scattering beamlines, needs to be developed for CENTAUR to provide interface for techniques such as spectrometry, in-beam size-exclusion chromatography, etc.
- **Sample staging capability:** A sample staging capability is needed for many samples to be ready from a storage condition to an experimental condition. Currently, a sample is typically staged in the beam position for equilibrium, resulting significant inefficiency in using neutron beam time. To minimize that, a sample staging capability will be implemented to allow upcoming samples to be ready while a current sample is being measured.
- **Specialized cells** such as pressure cell, gas-loading cell, relative humidity cell, shear cell, etc.: with smaller sample requirements, additional improvements on those specialized sample cell are needed to take full advantage of CENTAUR.

2.9.5 MAGNETISM EXPERIMENT

With the polarization system, CENTAUR will provide an ideal place for studying magnetism. The provisions have been made to accommodate all existing cryo-magnets that are typically used in the SANS experiment, e.g., Mag-G 11 T, Mag-H 5 T. A large capacity goniometer will be in sample position to tilt and align magnets. An upper floor will provide easy access for those sample environment (Figure 11).

2.10 INFRASTRUCTURE & UTILITIES (WBS: S04.07.09)

CENTAUR will have the infrastructure items in common with the majority of beamlines. The instrument will be equipped with utilities such as Sensible Chilled Water, Process Water, Compressed Air, and Electrical Power. CENTAUR will be evaluated with ES&H personnel to determine the location of sprinkler system, smoke detectors, fire alarms, radiation sensors, etc. Additionally, standard Personnel Protection System (PPS) and Oxygen Deficiency Hazard (ODH) equipment will be provided as required. Further development of instrument is required to determine best location of safety equipment and instrument utilities.

CENTAUR's control hutch will be located on the 2nd floor of the instrument. It will house workstation equipment and be furnished providing a dedicated workspace for users. In addition, the location of the hutch will provide closer access to building mezzanine.

CENTAUR's detector system requires for its electronics to be mainainted at a constant temperature, reducing temperature fluctuations. Part of the Detector R&D effort will involve studying heat dissipation of the new SiPM Anger camera configuration. The detector cooling system infrastructure will be designed to ensure it meets detector cooling specifications taking into account any R&D findings.

To facilitate the monitoring of CENTAUR's complex sample environments, infrastructure equipment, such as video cameras, will be included to remotely observe sample and sample environments during neutron experiments.

To ensure samples are properly handled, CENTAUR will include a sample preparation space and Radiation Material Area (RMA) near the instrument. Having items in close proximity to instrument will be imperative for sensitive samples.

2.11 INSTRUMENT CONTROLS AND DAQ (WBS S06.04.07) & SCIENTIFIC SOFTWARE (WBS: S04.02)

As a high-throughput instrument with a broad user community with both expert and non-expert users, the instrument control software and scientific software needs are very expansive and critical for science success. Here we laid out addtional considerations forCENTAUR. Remote experiment access has been implemented at ORNL neutron facilities. CENTAUR needs to conform to facility remote experiment requirements with the consideration that a significant number of users will request this mode for instrument access.

- A significant portion of experiment (20-30 %) is high-throughput measurement with relatively standard instrument configurations. Remote experiments will likely be the main access mode for such experiments, a standard sample cassette or holder with automatic sample recognition system such as barcodes will be developed to reduce the burden of users and facility.
- Instrument control and data acquisition system (IC&DAS) will be developed to enable the remote access capability.
- IC&DAS needs different user interaction interfaces to accommodate different user communities and user expert-levels. For example, a scripting interface will provide highest flexibility in expert users to setup complex experiment, while a wizard-like interface is needed to setup relative routine scans.
- Automatic data reduction converting the data into Q space, which is most SANS data being used scientifically in the community, needs to be implemented. This conversion should be in real-time or near real-time to facilitate effective experiment steering by users or artificial intelligence. Users can always re-reduce data as needed after the experiment.
- Automatic data analysis, when appropriate, needs to be performed. For example, for many solution scattering or diffraction experiments, rudimentary analysis such as Guinier, power-law, pair distribution function, etc. should be performed automatically once the auto data reduction is performed.
- The raw data, automatic reduced data, and automatic data analysis needs to be visualized effectively.
- Given the much higher data rate and data volume, effective mechanisms are needed for quick data/ meta-data storage, cataloguing, and retrieval.
- The instrument control and scientific software should have expandability to plug in additional functionality from future development such as new analysis methods, machine learning methods, etc.

2.12 PERFORMANCE ESTIMATION

The instrument simulations were performed using Monte Carlo packages McStas[34] or MCViNE[35] for SANS/WANS/diffraction or spectrometry, respectively. The positions of the components were as described in the previous sections, using suitable gaps to represent spaces between the guides and other optical components. At present, no component exists for the T0 choppers to be used at the STS. As a result, the position was left as an empty gap in the Monte Carlo model. The performance estimation is based on STS source file *BL6-Tube-90D-STS-Min-2G-source_mctal-55_sp.dat* (2021).

2.12.1 DATA ON DETECTOR AND Q SPACE

As mentioned previously, the sample geometry used in the simulation is plate at least 10 mm by 10 mm with thickness of 1 mm, with the sample aperture of 5mm in radius. As SANS are applicable to almost any sample morphology and in any state, here two samples from McStas 2.7 SANS_benchmark2 component, a monodispersed sphere with 25Å radius (no. 5) and sharp peaks (no.11) are presented to represent medium to high-feature samples.

The scattering pattern of the sphere on the position sensitive detectors at different arrays are shown in Figure 12. The sharp feature from the scattering is smeared by the wide wavelength band, as in

any TOF SANS instrument. But converting them into Q space (Figure 13) reveals the form factor of a sphere scattering well. The Q range from different arrays also overlap well. The difference in Q resolution at different detector array can be seen at the first dip near 0.1 Å^{-1}, where the high-angle array data is less sharp than the other two, but otherwise not visible for this sample.

Backscattering   High-angle   Mid-angle   Low-angle

Figure 12. Detector raw data from simulation on a sphere of 25Å (NG=3, wavelength band 2-9.43Å). No sharp feature can be seen due to TOF data. The shadow on the low-angle detector is the shadow of the beam trap. The backscattering detectors registered few neutrons due to the sample. Its performance was tested in 2.2.4 with a more diffraction-like sample.
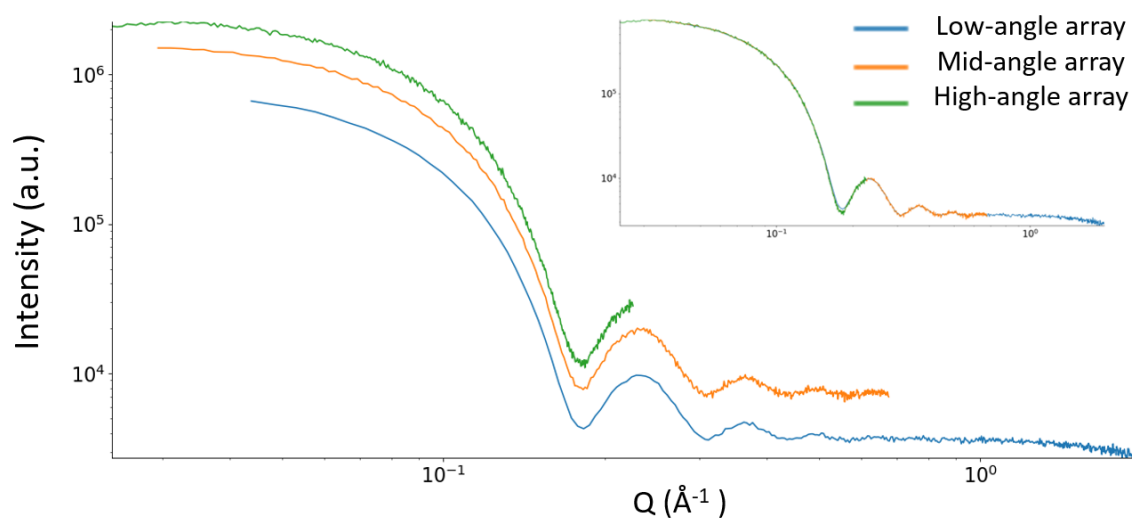

Figure 13. Simulated data from a sphere of 25 Å in radius in I vs. Q 1D curve. They are offset for clarity. The inset is a view of all detector data merged.
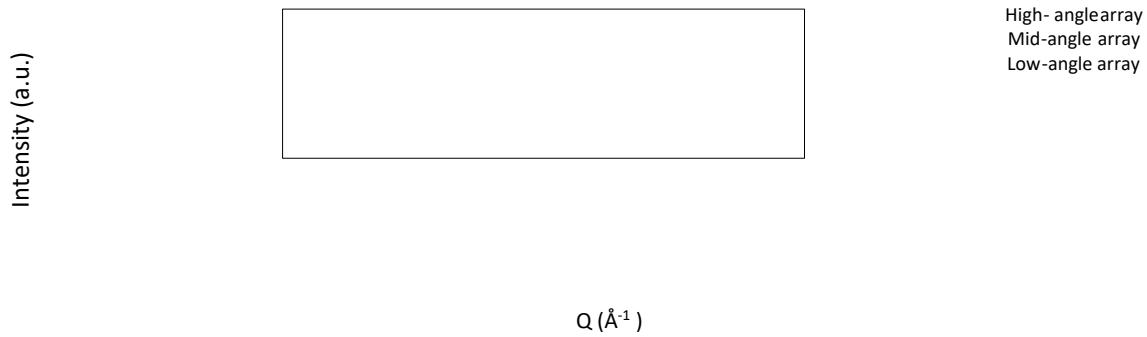
Figure 14. Simulated scattering with sharp peaks at three forward detector arrays (15 Hz, 1-8.43 Å NG=0). The inset is the enlarged region between ~0.2 – 1.0 Å^{-1} to show the broadening of the same peak at different detectors due to different instrument geometry resolution at different detector arrays.

The instrument resolution changes due to the sample-to-detector distance can be seen more clearly from the simulation on a sample with sharp peaks in Figure 14. For example, the FWHM of the 0.215 Å^{-1} peak on the high-angle detector is about twice of the mid-angle detector, while the mid-angle detector and low-angle detector are similar with < 10% $\Delta Q/Q$ as required by most science cases. In this case, if higher resolution is preferred, the high-angle detector data should be discarded to just use the Q range from other detectors. However, it is worth noting that instead of fitting a stitched data set from different detectors, multiple datasets from different detector arrays can be fitted simultaneously with different instrument resolution functions to take advantage of this wealth of the data in the future.

With different collimation distance, the instrument resolution (in terms of different NG) impacts the features of the scattering, as shown by peak broadening in Figure A2 in Appendix A. However, the impact of different resolution for a typical SAS sample with little sharp feature is limited. And the flexibility in collimation configuration provides a means to increase resolution with reduced flux.

2.12.2 FLUX AT SAMPLE

The integrated flux estimates at the sample position for representative configurations at both potential operating frequencies were also calculated from the McStas simulation results and are presented in Table 5. As shown, the flux at those configurations is very good, compared with the existing SNS and High Flux Isotope Reactor (HFIR) SANS instruments (Table A1 in Appendix A) with orders-of-magnitude improvement in both flux and Q range. Specifications from additional similar instruments from other major user facilities are also listed in Table A1 in Appendix A for comparison. The performance of CENTAUR, in term of dynamic Q range (Q_{max}/Q_{min}) and flux, will be truly exceptional.

Table 5. CENTAUR Q range and flux at sample at selected instrument configurations. The Q range from the forwarding detectors (3 arrays combined) and backscattering detectors are listed separately. The Q range is calculated by using corresponding scattering angle 2θ with λ_{min} and λ_{max} for Q_{max} and Q_{min}, respectively.

Configuration	Wavelength range (Å)	Q-range (Å^{-1}) (forwarding detectors)	Q range (Å^{-1}) (backscattering detector)	Flux at sample, (n/s/cm^2)
15 Hz, NG=0	2.00–9.43	0.0016–1.9	1.4–6.25	7.17E7
15 Hz, NG=1	2.00–9.43	0.0023–1.9	1.4–6.25	1.39E8

15 Hz, NG=2	2.00–9.43	0.0039–1.9	1.4–6.25	4.03E8
15 Hz, NG=3	2.00–9.43	0.0056–1.9	1.4–6.25	6.89E8
15 Hz, NG=0	1.00–8.43	0.0018-3.8	1.25–13.50	8.04E7
15 Hz, NG=1	1.00–8.43	0.0026-3.8	1.25–13.50	1.56E8
15 Hz, NG=2	1.00–8.43	0.0044-3.8	1.25–13.50	4.49E8
15 Hz, NG=3	1.00–8.43	0.0063–3.8	1.25–13.50	7.63E8
7.5 Hz, NG=0	0.50–15.36	0.001–5.86	0.83–25.0	4.24E7
7.5Hz, NG=3	0.50–15.36	0.0035–5.86	0.83–25.0	3.99E8

2.12.3 BRILLIANCE TRANSFER AND DIVERGENCE

The brilliance transfer and divergence are obtained based on a sample of 5 mm in radius. For example, when all neutron guides are in place (NG=3), the maximum divergence is ±0.39° (full peak width) (Figure 15A). When all the neutron guides are removed from the collimation section, providing the highest collimated beam, the maximum divergence is ±0.10° (Figure 15B). The maximum divergences are ±0.17° and ±0.25° for NG=1 and 2, respectively (Figure 15C). The brilliance transfer is calculated based on the sample phase space in Figure 15D.
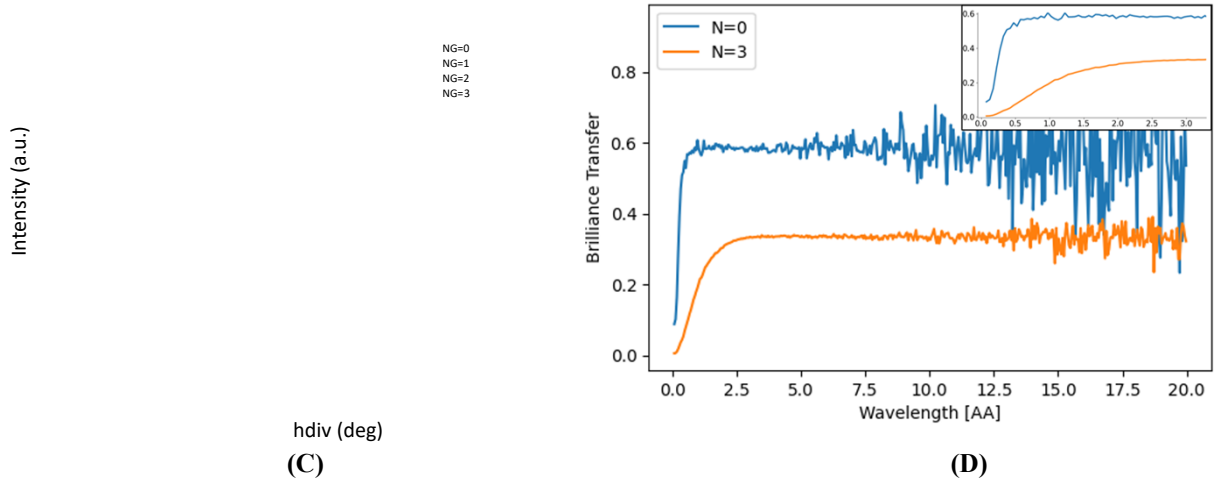

(A)

(B)
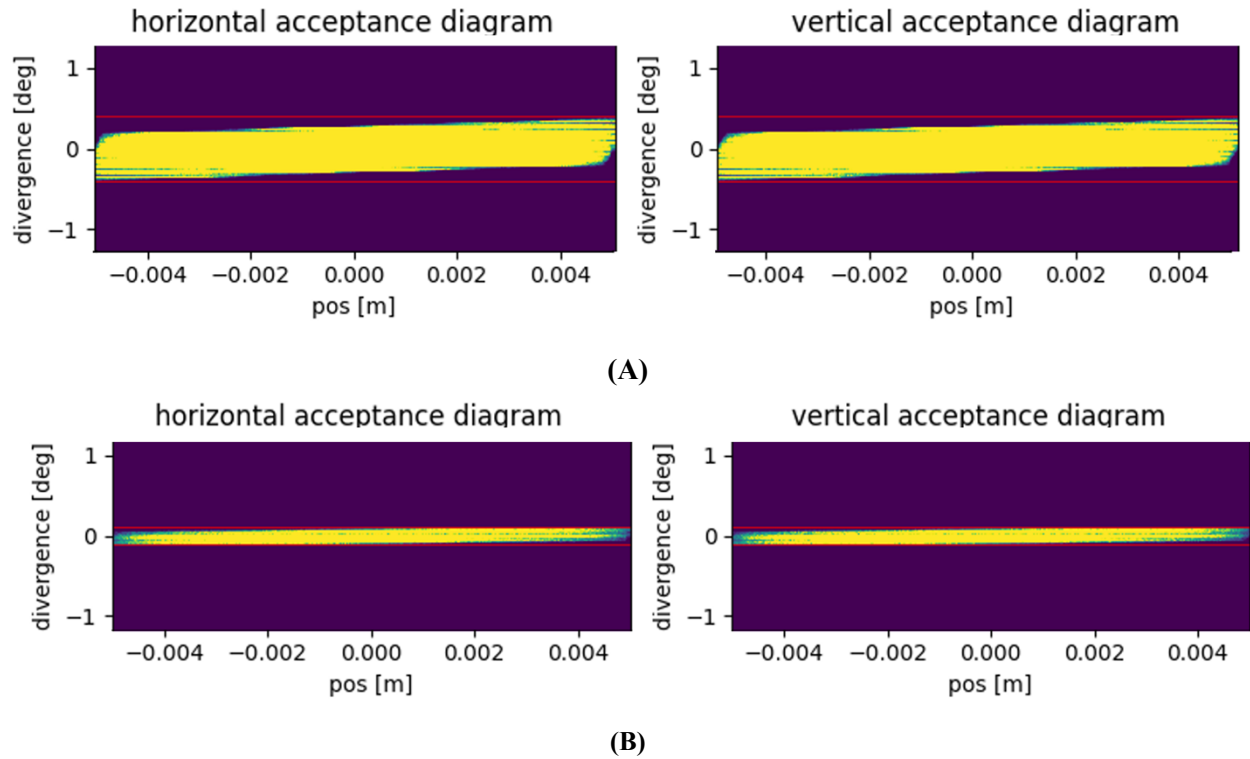
Figure 15. Phase space limit of sample at all guides (A) NG=3 and zero guide (B) NG=0. (C) Maximum divergence at the sample position. (D) the brilliance transfer for NG=0 and NG=3. The inset enlarges on the shorter wavelengths.

2.12.4 DIFFRACTION ON THE BACKSCATTERING DETECTORS

The diffraction resolution $\Delta Q/Q$ on the backscattering detectors is evaluated with a pseudo-polycrystalline sample with sharp peaks up to 15 Å^{-1} in flat geometry with a thickness of 1mm. NG=0 (best collimation) and NG=3 (highest flux at the sample) with 15 Hz (wavelength band 2–9.43 Å) and 7.5 Hz (wavelength band 0.50–15.43 Å) configurations were tested (Figure 16 and Figure A1 in Appendix A). The Q resolution $\Delta Q/Q$ was estimated from the ratio between the full width at half maximum (FWHM) of the diffracted peaks and the peak location (Q). From the results, $\Delta Q/Q$ was found to be between 0.025% and 0.89%, satisfying the science-driven requirement of less than 1%. The backscattering geometry at CENTAUR provides good diffraction capability.

Figure 16. Diffraction peaks measured at 7.5 Hz, NG=3 on the backscattering detector array. The inset enlarges on the higher Q region.

2.12.5   DIRECT GEOMETRY SPECTROMETER PERFORMANCE EVALUATION

Taking advantage of the time-of-flight source, CENTAUR can be transformed to serve as a direct geometry spectrometer (DGS) by inserting a high-speed Fermi chopper before the sample position, as described in the key instrument component. Among the three detector arrays, the arrays at 1.111 m and 3.333m are similar to other DGS, e.g., CHESS, but with much smaller detector angular coverage. But the low-angle detector array at 10 m will provide a capability to measure very small energy and momentum transfer, filling a gap of typical DGS as an inelastic SANS instrument. The dynamic range at the 10 m detector in momentum transfer (Q) and energy transfer ($\Delta E=E_i-E_f$) is shown in Figure 17A in the range of incident energy 0.5–500meV (12–0.4 Å).

As an addon feature, the optimization of DGS is constrained by other priorities, with only the optional chopper as the parameter. But similar to other cold neutron spectrometers, CENTAUR aims to provide a good energy resolution at lower energy, for example, ~1% with E_i=2 meV, which needs the burst time of the high-speed chopper to be ~30 µs. The instrument performance was estimated with a high speed chopper burst time of ~30 µs in the MCViNE software.[35] The instrument was set to use all neutron guides (NG=3) to maximize flux at the sample position. and 2.8 m in front of the sample position, providing a decent flux at the sample position (Figure 17B) over the energy range. Using samples with different fixed momentum transfer and energy transfer, the inelastic scattering data were collected at the 10 m detector array and then reduced into momentum transfer (Q) vs. energy transfer ($\Delta E=E_i-E_f$). The instrument resolution at different incident energies (E_i=2, 5, 80 meV) was then obtained by measuring the FWHM of the inelastic peak in Q-ΔE plot (Figure 18). The result was consistent with calculations from the inelastic resolution equation[36] with a nominal detection uncertainty time, as shown by the dashed line in Figure 18. The specification of a Fermi chopper is currently underway. The inelastic energy resolution and flux can be further adjusted by different Fermi chopper settings.
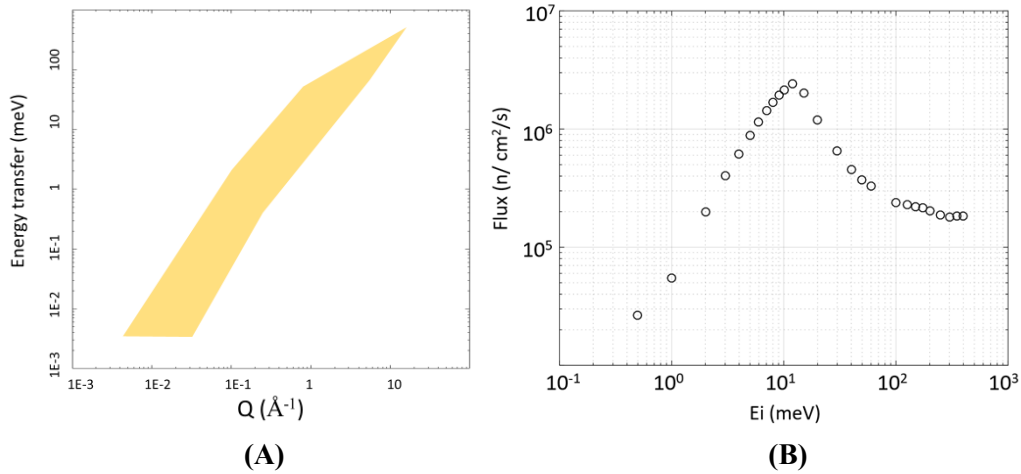

(A)   **(B)**

Figure 17. (A) The dynamic range in energy transfer and Q covered by the CENTAUR 10 m detector with incident energy E_i from 0.5 to 500meV (12-0.4 Å) (B)Flux at the sample position with different incident energy (NG=3).
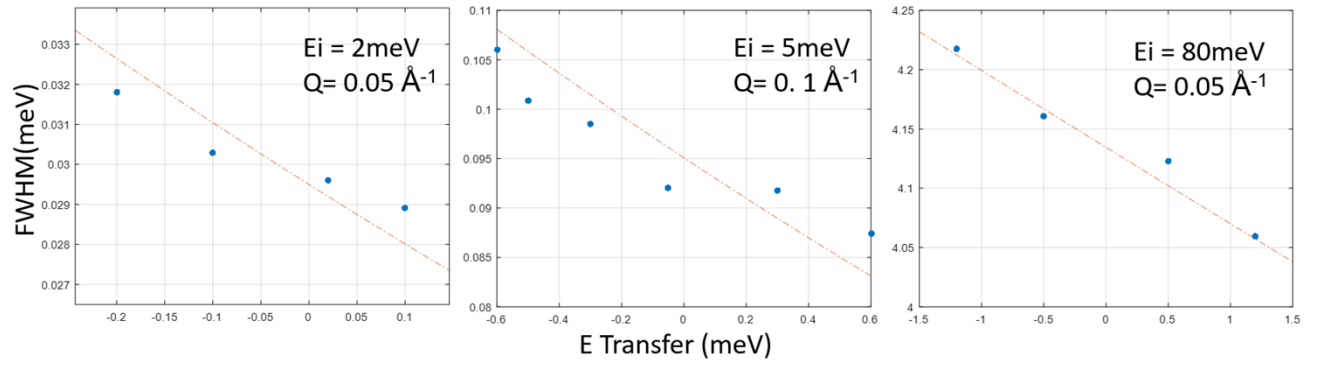
Figure 18. The inelastic energy resolution from MCViNE simulation at the CENTAUR 10 m detector array at various incident energies (Ei) as labeled. The samples were fixed in momentum transfer (Q) as shown and were varied in energy transfer. The dots are from the MCViNE simulation; the dashed line was calculated from the inelastic resolution function from [36]

Bibliography

1. National Academies of Sciences, E. *Frontiers of Materials Research: A Decadal Survey*. (2019). doi:10.17226/25244.
2. NSF. Frontiers in Polymer Science and Engineering (workshop report). (2016).
3. Challenges at the Frontiers of Matter and Energy: Transformative Opportunities for Discovery Science A REPORT FROM THE BASIC ENERGY SCIENCES ADVISORY COMMITTEE. (2015).
4. Gong, J. P., Katsuyama, Y., Kurokawa, T. & Osada, Y. Double-Network Hydrogels with Extremely High Mechanical Strength. *Advanced Materials* **15**, 1155–1158 (2003).
5. Okumura, Y. & Ito, K. The Polyrotaxane Gel: A Topological Gel by Figure-of-Eight Cross-links. *Advanced Materials* **13**, 485–487 (2001).
6. Tang, J., Sun, W., Tang, H., Radosz, M. & Shen, Y. Enhanced CO2 Absorption of Poly(ionic liquid)s. *Macromolecules* **38**, 2037–2039 (2005).
7. Supasitmongkol, S. & Styring, P. High CO2 solubility in ionic liquids and a tetraalkylammonium-based poly(ionic liquid). *Energy Environ. Sci.* **3**, 1961–1972 (2010).
8. Aghaie, M., Rezaei, N. & Zendehboudi, S. A systematic review on CO2 capture with ionic liquids: Current status and future prospects. *Renewable and Sustainable Energy Reviews* **96**, 502–525 (2018).
9. Zeng, S. *et al.* Ionic-Liquid-Based CO2 Capture Systems: Structure, Interaction and Process. *Chem. Rev.* **117**, 9625–9673 (2017).
10. Snæbjörnsdóttir, S. Ó. *et al.* Carbon dioxide storage through mineral carbonation. *Nature Reviews Earth & Environment* **1**, 90–102 (2020).
11. Clarkson, C. R. *et al.* Pore structure characterization of North American shale gas reservoirs using USANS/SANS, gas adsorption, and mercury intrusion. *Fuel* **95**, (2012).
12. Ruppert, L. F. *et al.* A USANS/SANS Study of the Accessibility of Pores in the Barnett Shale to Methane and Water. *Energy Fuels* **27**, 772–779 (2013).
13. Zhang, R. *et al.* Estimation and modeling of coal pore accessibility using small angle neutron scattering. *FUEL* **161**, 323–332 (2015).
14. Sang, G., Liu, S., Elsworth, D., Zhang, R. & Bleuel, M. Pore-Scale Water Vapor Condensation Behaviors in Shales: An Experimental Study. *TRANSPORT IN POROUS MEDIA* **135**, 713–734 (2020).
15. Liu, S. & Zhang, R. Anisotropic pore structure of shale and gas injection-induced nanopore alteration: A small-angle neutron scattering study. *International Journal of Coal Geology* **219**, 103384 (2020).
16. Zhang, R. & Liu, S. Nanoscale Coal Deformation and Alteration of Porosity and Pore Orientation Under Uniaxial Compression: An In Situ SANS Study. *Rock mechanics and rock engineering* (2021) doi:10.1007/s00603-020-02321-x.
17. Stefanopoulos, K. L. *et al.* Neutron Scattering Measurements of Carbon Dioxide Adsorption in Pores within the Marcellus Shale: Implications for Sequestration. *Environ. Sci. Technol.* **51**, 6515–6521 (2017).
18. Eberle, A. P. R. *et al.* Direct Measure of the Dense Methane Phase in Gas Shale Organic Porosity by Neutron Scattering. *Energy Fuels* **30**, 9022–9027 (2016).
19. Melnichenko, Y. B. *Small-Angle Scattering from Confined and Interfacial Fluids: Applications to Energy Storage and Environmental Science*. (Springer International Publishing, 2016). doi:10.1007/978-3-319-01104-2.
20. Mitrea, D. M. & Kriwacki, R. W. Phase separation in biology; functional organization of a higher order. *Cell Communication and Signaling* **14**, 1 (2016).
21. Nickels, J. D. *et al.* The in vivo structure of biological membranes and evidence for lipid domains. *PLOS Biology* **15**, e2002214 (2017).

22. F. Semeraro, E., Marx, L., K. Frewein, M. P. & Pabst, G. Increasing complexity in small-angle X-ray and neutron scattering experiments: from biological membrane mimics to live cells. *Soft Matter* **17**, 222–232 (2021).
23. Liberton, M. *et al.* Probing the consequences of antenna modification in cyanobacteria. *Photosynth Res* 1–8 doi:10.1007/s11120-013-9940-0.
24. Liberton, M. *et al.* Organization and Flexibility of Cyanobacterial Thylakoid Membranes Examined by Neutron Scattering. *J. Biol. Chem.* **288**, 3632–3640 (2013).
25. Back, C. *et al.* The 2020 skyrmionics roadmap. *J. Phys. D: Appl. Phys.* **53**, 363001 (2020).
26. Nagaosa, N. & Tokura, Y. Topological properties and dynamics of magnetic skyrmions. *Nature Nanotechnology* **8**, 899–911 (2013).
27. Kautzsch, L., Bocarsly, J. D., Felser, C., Wilson, S. D. & Seshadri, R. Controlling Dzyaloshinskii-Moriya interactions in the skyrmion host candidates ${\mathrm{FePd}}_{1\ensuremath{-}x}{\mathrm{Pt}}_{x}{\mathrm{Mo}}_{3}\mathrm{N}$. *Phys. Rev. Materials* **4**, 024412 (2020).
28. Bocarsly, J. D., Need, R. F., Seshadri, R. & Wilson, S. D. Magnetoentropic signatures of skyrmionic phase behavior in FeGe. *Phys. Rev. B* **97**, 100404 (2018).
29. Gao, S. *et al.* Fractional antiferromagnetic skyrmion lattice induced by anisotropic couplings. *Nature* **586**, 37–41 (2020).
30. Sala, G., Lin, J. Y. Y., Graves, V. B. & Ehlers, G. Conceptual design of CHESS, a new direct-geometry inelastic neutron spectrometer dedicated to studying small samples. *J Appl Cryst* **51**, 282–293 (2018).
31. Sette, F. *et al.* Collective Dynamics in Water by High Energy Resolution Inelastic X-Ray Scattering. *Phys. Rev. Lett.* **75**, 850–853 (1995).
32. Mamontov, E. *et al.* Water dynamics in a lithium chloride aqueous solution probed by Brillouin neutron and x-ray scattering. *J. Phys.: Condens. Matter* **24**, 064102 (2012).
33. Wang, T. *et al.* New Polarized Small Angle Neutron Scattering capability at the High Flux Isotope Reactor. *Physica B: Condensed Matter* **551**, 492–495 (2018).
34. Willendrup, P., Farhi, E., Knudsen, E., Filges, U. & Lefmann, K. McStas: Past, present and future. *Journal of Neutron Research* **17**, 35–43 (2014).
35. Lin, J. Y. Y. *et al.* MCViNE – An object oriented Monte Carlo neutron ray tracing simulation package. *Nuclear Instruments and Methods in Physics Research Section A: Accelerators, Spectrometers, Detectors and Associated Equipment* **810**, 86–99 (2016).
36. Ehlers, G., Podlesnyak, A. A., Niedziela, J. L., Iverson, E. B. & Sokol, P. E. The new cold neutron chopper spectrometer at the Spallation Neutron Source: Design and performance. *Review of Scientific Instruments* **82**, 085108 (2011).
37. Jaksch, S. *et al.* Concept for a Time-of-Flight Small Angle Neutron Scattering Instrument at the European Spallation Source. *Nuclear Instruments and Methods in Physics Research Section A: Accelerators, Spectrometers, Detectors and Associated Equipment* **762**, 22–30 (2014).
38. Jackson, A. & Kanaki, Kalliopi. ESS Construction Proposal: LoKI - A broad-band SANS instrument. (2013).

APPENDIX A. ADDITIONAL TABLES AND FIGURES

Table A1 Other major SANS instrument specifications. The instrument specifications from non-ORNL instruments are pulled from websites or references for other facilities.

| EQ-SANS (single detector, SNS)	Wavelength range (Å)	Q range (Å^{-1})	Flux at sample, (n/s/cm^2)
EQ-SANS, 4 m, 60 Hz	2.00–5.64	0.008–0.412	1.26E+7
EQ-SANS, 8 m, 60 Hz	10.00–12.98	0.002–0.041	2.53E+4
Bio-SANS (dual-detector, HFIR)			
7 guides, 2.25 m	6 Å Δλ/λ=0.14	0.010–1.00	2.00E+7
4 guides, 7 m	6 Å Δλ/λ=0.14	0.007–0.90	2.50E+6
0 guides, 15.5 m	6 Å Δλ/λ=0.14	0.003–0.85	1.01E+6
0 guides, 15.5 m	18Å Δλ/λ=0.14	0.001–0.20	1.50E+4
GP-SANS (single detector, HFIR)			
7 guides, 1.1 m	4Å Δλ/λ=0.144	0.051–0.962	3.31E+7
4 guides, 8.8 m	4Å Δλ/λ=0.14	0.0064–0.152	7.90E+6
0 guides, 19.3 m	18Å Δλ/λ=0.14	0.00095–0.0176	9.70E+3
TAIKAN (JPAC)			
25 Hz unpolarized neutron	0.5–8	0.005–20	N/A
25 Hz polarized neutron	0.5–8	0.005–2.5	N/A
iMATERIA (JPAC) 25Hz			
DF mode	0.5–8	0.007–34.7	N/A
SF mode	0.5–8	0.014–34.7	N/A
VSANS 30m (NIST NCNR)			
	12	0.0002–0.375	N/A
	4.5	0.0053–1	N/A
SKADI (ESS, to be built)[37]			
	2–13	0.0001–1	~ 1E+8
LoKI (ESS, to be built)[38]			
5 mm sample diameter, 10 m source distance	3–10.5	0.0009–1.66	1.27E+7
10 mm sample diameter, 2 m source distance	3–-10.5	0.00768–1.66	9.73E+8

Intensity (a.u.)

Q (Å⁻¹)

(A)

Intensity (a.u.)

Q (Å⁻¹)

(B)

Intensity (a.u.)

Q (Å⁻¹)

(C)
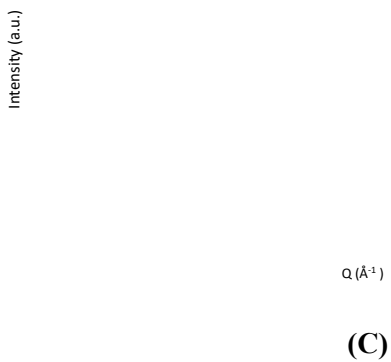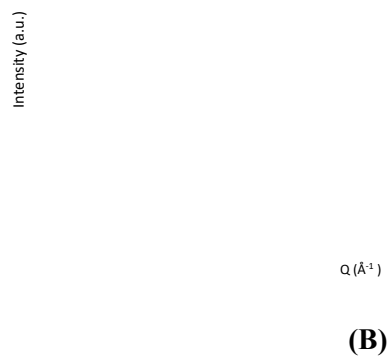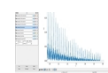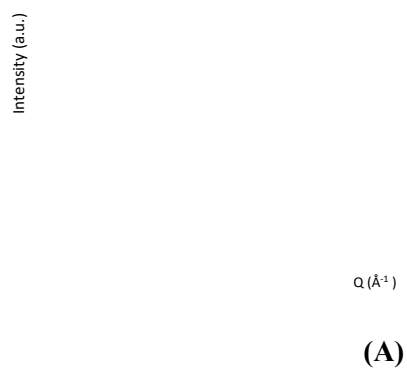
Figure A1. Diffraction peaks measured at (A) 15 Hz, NG=3, (B) 7.5 Hz, NG=0, (C) 15 Hz, NG=0 on the backscattering detector array. The inset is enlarged on the higher Q region.
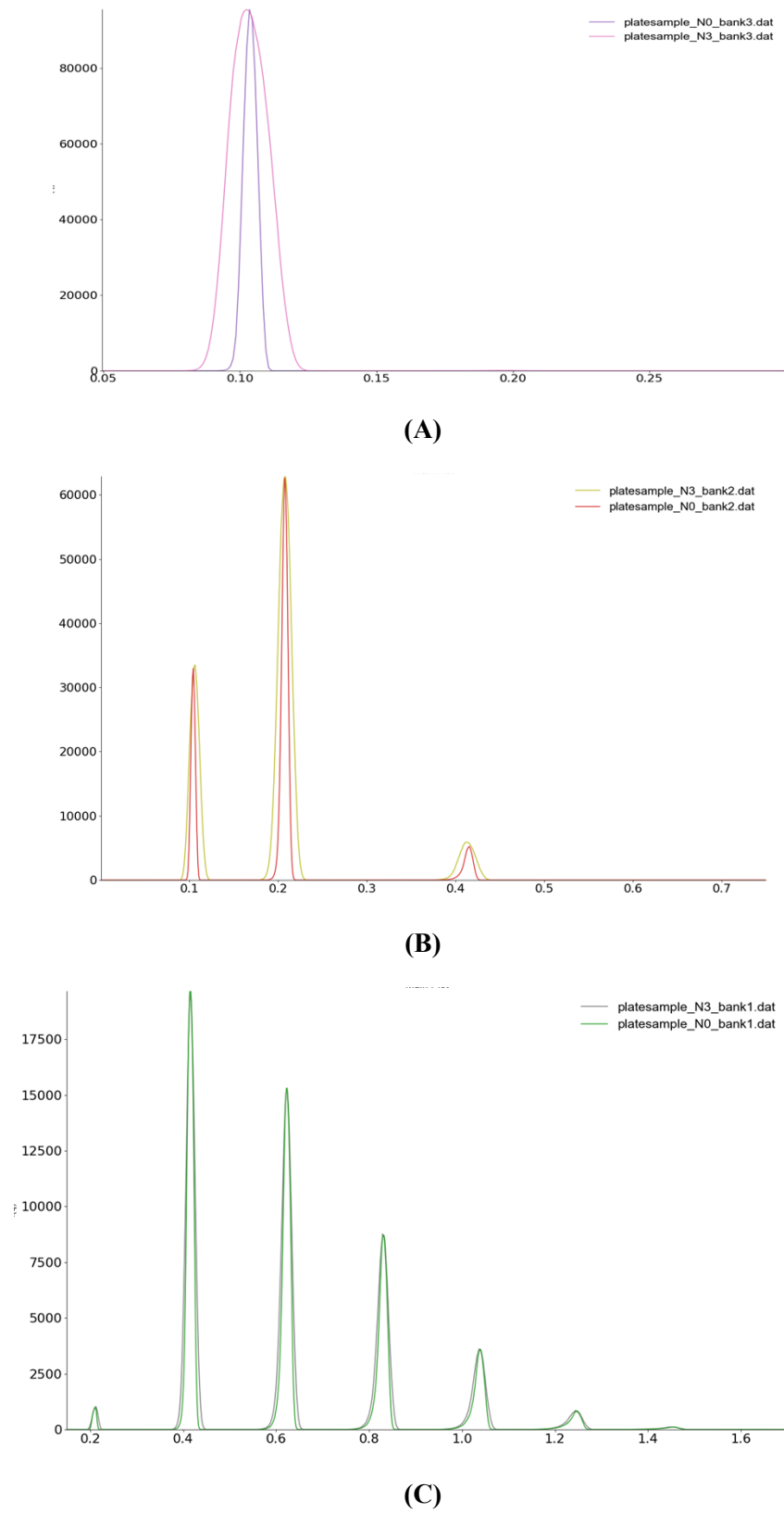
(A)

(B)

(C)

Figure A2. The peak broadening caused by different collimation distances (N0 is 10 m, and N3 is ~3 m) at different detector arrays: (A) low-angle array, (B) mid-angle array, (C) high-angle array

APPENDIX B. MCSTAS CODE:

The separate file is attached for this: APP. B centaur20220302.pdf

APPENDIX C. MCVINE CODE

The seperature file is attached for this: App. C dgs_tube_centaur.pdf